第27卷 第5期
2006年 10月

材 料 热 处 理 学 报
TRANSACTIONS OF MATERIALS AND HEAT TREATMENT

Vol. 27 No. 5
October 2006

TiAl 合金微弧氧化膜的制备及抗氧化性能研究

李夕金[1]， 程国安[1]， 薛文斌[1]， 郑瑞廷[1]， 吴晓玲[1]， 程云君[2]

(1. 北京师范大学材料科学与工程系射线束技术及材料改性教育部重点实验室，北京 100875；
2. 钢铁研究总院 TiAl 系金属间化合物研究中心，北京 100081)

摘 要：利用微弧氧化的方法在γ-TiAl 合金上制备陶瓷膜，探讨了氧化过程中电流密度与成膜速度的关系。利用扫描电镜研究了氧化膜的表面形态和截面结构，结果表明，氧化膜由三层组成，且氧化膜与基体间有良好的冶金结合；物相分析发现氧化膜中含有金红石、Al_2TiO_5 和 SiO_2 非晶成分，并且物相组成和分布与成膜时间及膜的深度无关；氧化膜的硬度随着氧化时间的增加而增加，极大值出现在距离膜基交界面约 10μm 附近的氧化膜中。1100 ℃下的高温氧化实验发现微弧氧化处理后样品的氧化速度只有原始基体材料的 1/3，微弧氧化处理后提高了 TiAl 合金的抗氧化性。

关键词：微弧氧化； TiAl； 显微硬度； 高温氧化

中图分类号：TG146.2； TG174.45 **文献标识码**：A **文章编号**：1009-6264(2006)05-0095-05

TiAl 合金由于其优异的性能，密度小，高温强度高，抗氧化性好和刚性好等，引起国内外广泛重视。但是钛铝合金的长期使用温度只有 600 - 650 ℃[1]，人们研究了多种表面处理的工艺和方法来提高钛铝合金的使用温度，如真空等离子喷涂[2]、激光表面合金化、渗铝[3]、表面涂层[4]、渗氮[5]、渗硼[6]等，以提高合金的抗氧化性。

微弧氧化是利用导体在电解液中微区等离子火花放电的方式在 Ti、Mg、Al 等金属表面生成一层氧化物陶瓷膜[7,8]。由于生成的陶瓷膜中金属离子来自基体，氧离子来自电解液，氧化膜的生长是一种原位生长方式，因而膜与基体间具有良好的结合强度。微弧氧化方法可以生成较大厚度的氧化膜，可用来达到提高抗氧化性和其它方面的改变材料性质的目的。利用微弧氧化技术在铝、镁等基体上生长陶瓷膜取得了较好的结果[9-11]，制得的陶瓷膜能够极大的改善材料的耐磨性，耐腐蚀，耐热冲击和绝缘性能。但在 TiAl 金属间化合物表面进行微弧氧化[12]，并制得可以实用的陶瓷膜的研究，目前进行的还较少。本实验采用微弧氧化技术在 TiAl 表面生成氧化膜，研究了氧化膜的硬度、耐高温性能、以及氧化前后的物相变化。

1 实验材料和方法

γ-TiAl 合金名义成分(at %)为 Ti-48Al-2Cr-2Nb，由γ-TiAl 相和少量的 α_2-Ti_3Al 相组成。样品经线切割加工，尺寸为 40mm ×12mm ×2mm，经 600 号砂纸打磨后进行微弧氧化处理。电源为自行研制的交流脉冲电源，其正负电压可以分别调节。通电后阳极电压逐步升到 600V，阴极电压为 - 200V。阳极电压达到 600V 后保持电压恒定。电解液成分为 Na_2SiO_3，加少量的 KOH 以调节电解液的 pH 值。整个氧化过程中保持电解液的温度不超过 50 ℃。氧化时间分别取为 7、30、60、120min。

微弧氧化制备的样品干燥后经涡流测厚仪测量氧化膜的厚度。基体、氧化膜表面以及氧化膜不同层内的物相分析由 X'PERT PRO MPD X 射线衍射仪(XRD)测得。用扫描电子显微镜(SEM Hathchi-4300)观察膜表面的形貌及氧化膜横截面的结构，并通过 SEM 所带的能谱仪(EDX)分析膜横截面内的元素分布。使用维氏显微硬度计(1000HV)测量膜的硬度分布，载荷为 10g。将 2h 微弧氧化的样品和基体分别放入电炉中加热，温度上升到 1100 ℃，保温时间分别为 10、20、40、60、80、100h。温度保持到设定时间后，将样品依次从炉中取出，自然冷却至室温，分别测量其氧

收稿日期： 2005-11-23； **修订日期**： 2006-03-13

基金项目： 国家自然科学基金资助项目(10575011)；北京市科技新星计划(9558102500)；北京市科学技术研究院萌芽计划

作者简介： 李夕金(1968—)，男，北京师范大学材料科学与工程系博士生，主要进行金属材料表面微弧氧化改性研究。电话：010-62205403，E-Mail：lxjzbj@126.com。

通讯作者： 吴晓玲(1972—)，女，北京师范大学材料科学与工程系讲师。电话：010-62207222；E-mail：wuxl@bnu.edu.cn。

化前后的质量,并利用 XRD 对氧化后的膜表面以及膜/基界面的物相进行了分析。

2 实验结果及讨论

2.1 电流密度及膜的厚度随微弧氧化时间的变化

电流密度和氧化膜的厚度随氧化时间的变化关系如图 1 所示,厚度曲线可分为明显的三个区域:厚度快速增长的 AC 段,缓慢增长的 CF 段,停止增长的 FG段。厚度曲线与电流密度曲线有很好的对应关系。电流密度曲线的 AB 段是从普通阳极氧化到微弧氧化的过渡阶段。样品放入电解液后,电流密度很快增加到最大值(24A/dm^2)。随着膜层的增厚,氧化膜的电阻增大,电流密度呈线性减少。BC 段为明亮的微弧放电阶段,样品表面火花明亮并且分布均匀,氧化膜厚度增加较快(2.3μm/min)。CD 段中电流密度变化不大(11 - 13A/dm^2),对应于样品表面的暗火花放电阶段,氧化膜继续增厚,但氧化膜增长的速率下降(0.67μm/min)。DE 段电流明显下降,由于电解液对氧化膜外层的溶解和氧化膜向内生长的共同作用,氧化膜的厚度基本保持不变(110μm)。可见,氧化膜的生长速率与电流密度的变化密切相关。通过调控电流密度可以较好的控制膜厚的变化。

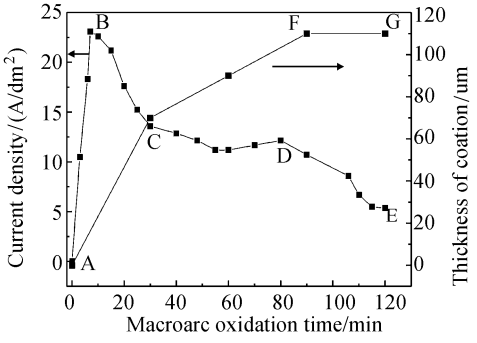

图 1 电流密度和氧化膜厚度随氧化时间的变化

Fig. 1 Dependence of the current density and the coating thickness with the MAO treating time

2.2 氧化物薄膜的表面形貌

不同微弧氧化时间的样品的表面形貌如图 2 所示,在各个不同的氧化阶段,放电孔成近似圆孔状,表面都表现为明显的熔融状态。图 2(a)显示样品表面不均匀,放电通道涌出的喷出物成点状稀疏沉积在样品表面。此时样品放入电解液 7min,只在样品表面有个别的稀疏的火花生成,火花分布不均匀。样品表面有火花出现的位置对应着图 2(a)中的熔融喷出沉积物的位置。图 2(b)所示为微弧氧化 30min 时的表面,放电孔数目较多、边缘清晰、分布均匀,喷出的熔融物沉积在放电孔周围。此时电解槽中样品表面的均匀明亮的火花刚刚消失,变为暗弱的小火花,开始转入暗火花放电阶段。图 2(c)为暗火花放电到 60min 时的表面形貌,表面的较大的放电孔道数目减少,单个放电孔的半径加大,同时出现大量的放电微孔。这是由于随着膜层的加厚,放电越来越困难,只有更高的电压才能击穿局部的氧化膜,因此放电孔减少,半径加大。同时由于小的放电火花的存在,不断出现的新的放电微孔。由于火花变小,溶液中离子经过电化学反应在表面的淀积更容易,淀积物也对原来形成的孔道进行填补,原来形成的放电孔被堵塞,使放电孔数目减少。图 2(d)为放电 120min 时,样品表面放电孔数目减少,粗糙度变大。这是由于放电火花更微弱,反应产物的淀积效应更明显的结果。

2.3 氧化膜横截面形貌及元素分布

对氧化膜的截面进行 SEM 分析,结果见图 3,氧化膜分为致密层,中间层,疏松层三层结构:致密层几乎没有孔洞,厚度 25 - 30μm;中间层约 40μm,其中有较多细小微孔出现;疏松层的厚度 30 - 50μm。各层之间的分界线不明显,过渡平缓,显示出各层之间结合良好。陶瓷膜与基体之间结合界面清晰,结构致密,表现为明显的冶金结合。

从图 3 中 Ti、Si、Al 的元素分布,可以看到较为清晰的元素分层结构:Ti 沿着膜层向外逐渐降低,出现明显的分层现象;Si 也出现明显的分层现象,但其分布与 Ti 相反,自内向外增加。可以清楚地看出,致密层中基本没有 Si 元素,而疏松层中有大量的 Si,却基本上不含 Ti。Si、Ti 两种元素在膜中呈现一种互补性分布。中间层内 Ti、Si、Al 的分布相对均匀。Al 元素从基体到膜的表面逐渐减少,其分布与 Ti 不同,直至氧化膜的表面还有 Al 元素出现。Al 的分布虽然不如 Ti、Si 的分层现象明显,但也显示出分层结构。

Si 来自溶液中的 SiO_3^{2-} 离子,通过扩散及放电通道进入氧化膜,在氧化膜内发生电化学反应而淀积。致密层中由于放电孔道细少,Si 离子无法进入。因此,Si 在膜中的分布与放电孔道的大小和数目密切相关。

2.4 氧化膜的物相分析

利用 XRD 分析了氧化时间 7、30 和 120min 的氧化膜以及 120min 氧化膜的致密层和疏松层的物相。由图 4 可见,不同氧化时间的氧化产物都是 R-TiO_2(金红石型)和 Al_2TiO(图 4(a),(b),(c))。图 4(a)是

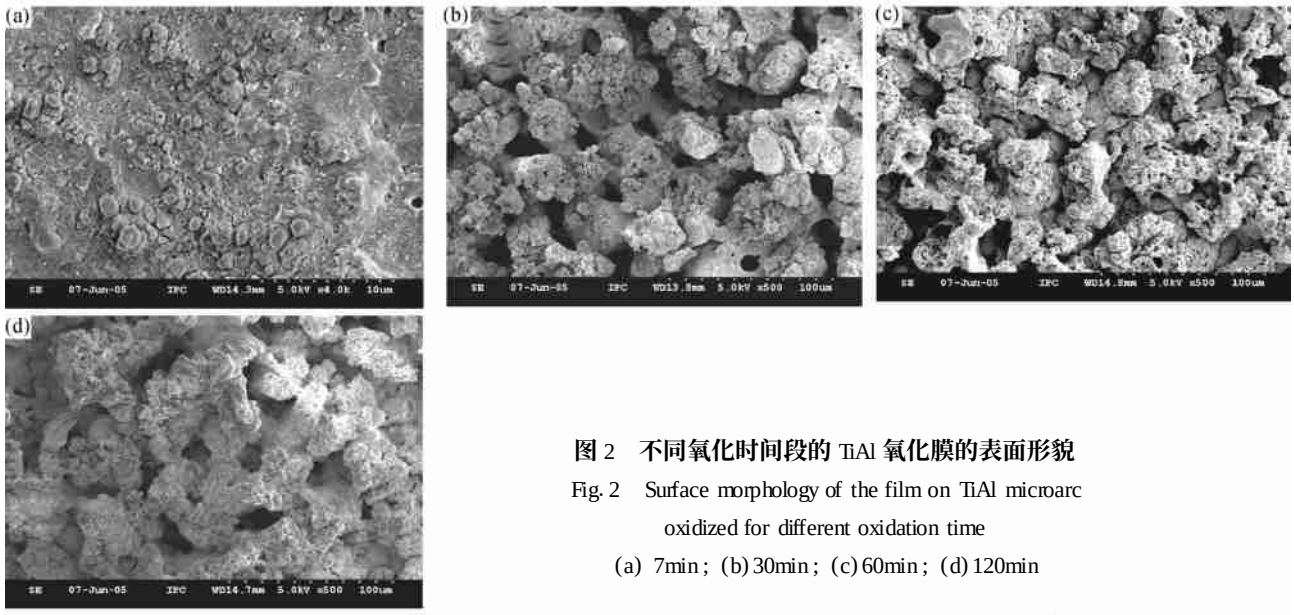

图 2　不同氧化时间段的 TiAl 氧化膜的表面形貌

Fig. 2　Surface morphology of the film on TiAl microarc oxidized for different oxidation time

(a) 7min; (b) 30min; (c) 60min; (d) 120min

氧化 7min 时的结果,其中有很强的基体相 TiAl 和 Ti_3Al 衍射峰出现,表明此时氧化膜很薄。随着氧化时间的增加,基体峰强度逐渐减小。微弧氧化 30min 时,基体峰消失,而 Al_2TiO_5 和 TiO_2 的峰明显增强。从 30min 到 120min 氧化膜中,致密层与疏松层只有 R-TiO_2 和 Al_2TiO_5 两种物相(图 4(c),(d)),比较致密层与疏松层的物相分析结果,可以明显看出致密层中 TiO_2 含量比高于疏松层中的含有量。与 30min 氧化膜相比,120min 氧化膜中的 Al_2TiO_5 的相对强度比 TiO_2 有所降低。

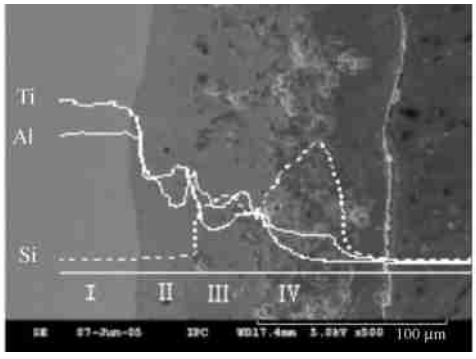

图 3　微弧氧化膜的截面结构及元素随深度变化

(I-基体; II-致密层; III-中间层; IV-疏松层)

Fig. 3　Microstructure and composition distribution of microarc oxidation films.

I-TiAl substrate; II-compact inner layer; III-intermediate layer; IV-loose outer layer

不同的氧化膜中都没有氧化硅晶体衍射峰出现,只有 2θ 角为 22°附近出现一个明显的 SiO_2 的非晶峰。但是从图 3 中可以发现,在氧化膜的表面有大量的 Si 存在。这表明在氧化膜中的 Si 元素以 SiO_2 的非晶形式存在,氧化膜的表面有大量的非晶 SiO_2,这一结论与 Al 合金微弧氧化膜的结论一致[13]。

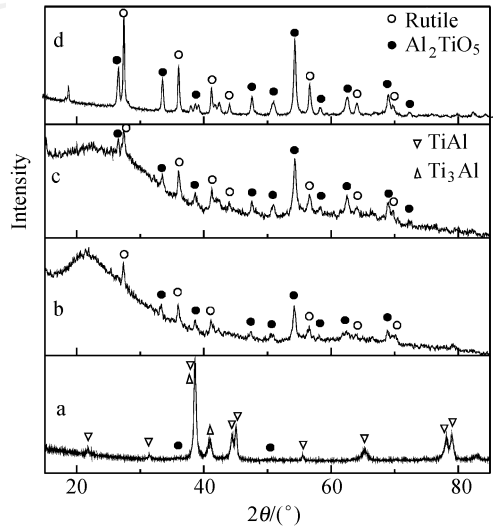

图 4　氧化膜的不同氧化时间的物相分析

(a) 7min; (b) 30min; (c) 120min; (d) 样品 c 的致密层

Fig. 4　XRD patterns of MAO films on TiAl alloys microarc oxidized for different time (a) 7min; (b) 30min; (c) 120min; (d) compact layer of (c)

TiAl 氧化首先生成 Al_2O_3 和 TiO_2,这两种氧化物在高温下进一步反应生成 Al_2TiO_5,因此在氧化膜中没有单独的 Al_2O_3 相存在,而 A-TiO_2(锐钛矿型)在 915 ℃可完全转变为 R-TiO_2[14]。XRD 分析显示氧化膜中只有 R-TiO_2 相出现,表明放电过程是一个高温过程。

2.5 氧化膜的硬度分析

显微硬度实验分别测量了微弧氧化时间为 30、60 和 120min 的氧化膜的显微硬度(图 5)。由硬度曲线可见,随着氧化时间的增加,氧化膜的平均硬度值增加。硬度曲线在距离膜/基体界面约 10μm 的位置出现一个峰值,同时注意到,随着氧化时间的增加,峰值向远离界面方向轻微移动。120min 氧化膜的硬度峰值达到 1350HV,是基体硬度值 450HV 的 3 倍。

影响膜硬度的因素主要有两个:膜的孔隙率和成分组成。随着膜的生长,致密层加厚,放电通道减少,致密层中的孔隙变少,致密度上升,使新生成的膜的硬度上升。另一方面,随着致密层的变厚,电解液中的 Si 不容易进入致密层,SiO_2 含量降低,致密层中超硬的 R-TiO_2 和 Al_2TiO_5 含量增加,也使氧化膜的硬度峰值上升。在氧化膜与基体交界处,不同氧化时间的氧化膜的硬度值变化不大。随着微弧氧化的进行,放电过程中的喷出物逐渐堵塞外围原来形成的放电孔道,使外部膜层中的孔道变少。因此在致密层变厚时,外部膜的硬度值有增大的趋势。

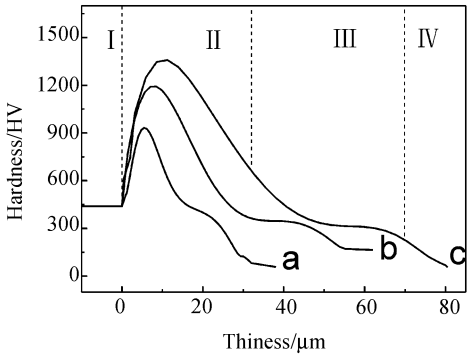

图 5 膜的硬度随距离变化 I基体 II致密层 III中间层 IV疏松层,(a),(b),(c)分别对应氧化时间 30,60,120min

Fig. 5 Microhardness profiles of the microarc oxidation films formed in different oxidation time
(a) 30min; (b) 60min; (c) 120min

2.6 高温氧化动力学

经过 100h 高温氧化实验曲线如图 6,氧化温度为 1100 ℃。基体的氧化曲线和 MAO 处理的样品的氧化曲线分为两部分。在前期,基体的热氧化速度(以质量的增加量表示)为 1.3×10^{-4} mg/mm^2,而微弧氧化处理的样品的热氧化速度仅为 1.6×10^{-5} mg/mm^2,比基体约低一个数量级。20h 后,基体的热氧化速度降为 1.2×10^{-5} mg/mm^2。而微弧氧化样品 60h 以后的氧化速度下降,几乎为零。经过 100h 高温热氧化后,微弧氧化样品的氧化速度只有基体的 1/3,可见微弧氧化膜较好的改善了 TiAl 合金的高温抗氧化性能。

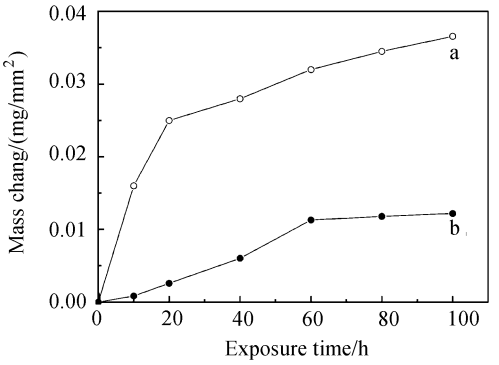

图 6 钛铝合金及微弧氧化样品在 1100 ℃下的氧化动力学曲线 (a)基体;(b)MAO 处理 2h

Fig. 6 Curves of isothermal oxidation kinetics of TiAl alloy and MAO film at 1100 ℃
(a) TiAl substrate; (b) MAO treatment 2h

XRD 分析发现,TiAl 基体高温氧化后的产物为 R-TiO_2 和 Al_2O_3(图 7(b))。微弧氧化处理样品经高温氧化后膜基之间的生成产物也是 R-TiO_2 和 Al_2O_3(图 7(a),(c)),但是原来存在于微弧氧化膜表面的非晶 SiO_2 在 1100 ℃温度下晶化(图 7(a))。将氧化膜剥离,对膜的背面进行 XRD 分析(图 7(c)),发现膜中 Al_2O_3 的相对含量低于基体氧化层的含量(图 7(b),(c))。

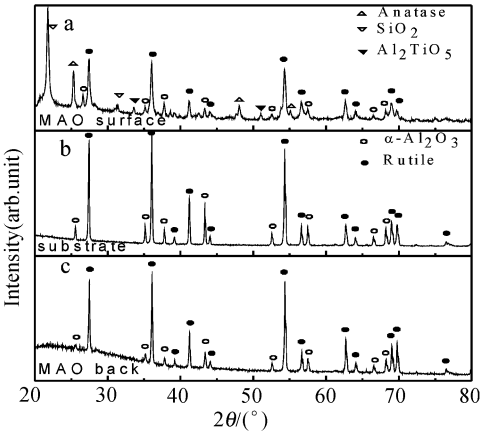

图 7 基体恒温氧化产物,MAO 样品恒温氧化产物 XRD 分析 (a)MAO 样品表面;(b)基体;(c)剥离的微弧氧化膜的背面

Fig. 7 XRD patterns of oxide after isothermal oxidation for substrate and MAO treated smaple

高温氧化前期,TiAl 基体无氧化膜保护,氧化速度较快,经 20h 热氧化后,表面形成较为完整的氧化

膜,阻碍了氧原子向基体的扩散,使氧化速度下降。而微弧氧化处理的样品由于膜的存在,阻碍了氧原子向膜内的扩散,使基体由于缺氧而缓慢氧化,因而氧化速度较小,60h 后进一步形成膜基间的热氧化膜,使氧化速度迅速降低。

微弧氧化样品中的 Al_2TiO_5 在 1100 ℃下容易分解为 TiO_2 和 Al_2O_3。由图 7(a),7(c) 可以看出,高温热氧化后的膜中的 Al_2TiO_5 含量已经很少,多数分解为 Al_2O_3 和 TiO_2。此外还有少量的 A-TiO_2 生成,可能是基体高温热氧化的产物。氧化膜表层中的非晶 SiO_2 经高温处理后晶化,衍射峰出现在 2θ 为 21.7 °附近。在高温热氧化初期,空气中的氧原子通过微弧氧化膜扩散与 TiAl 基体反应,在微弧氧化膜和基体之间生成 R-TiO_2 和 Al_2O_3。但氧原子的扩散受到微弧氧化膜的阻碍,氧化速度比无膜保护的基体的氧化速度小。随着氧化时间的延长,Al_2TiO_5 分解后的产物与膜基界面的热氧化产物相互作用,使后期氧化速度变得非常小。

3　结论

1) 氧化膜表面呈现通常的熔融状态,随着氧化时间的增加,放电孔的数目变少,残余的放电孔半径变大,整体粗糙度增加;

2) 在本实验条件下 TiAl 微弧氧化膜最大厚度为 110μm。前期生长阶段的平均速率为 2.3μm/min,后期生长阶段的平均速率为 0.67μm/min;

3) 氧化膜分为明显的三层结构:致密层,中间层,疏松层。致密层中 Si 含量极少,由 R-TiO_2 和 Al_2TiO_5 构成,疏松层中除含有 R-TiO_2 和 Al_2TiO_5 外,还有大量的 SiO_2 非晶相。氧化膜中没有单独 Al_2O_3 存在。氧化膜和基体之间呈现良好的冶金结合;

4) 微弧氧化膜的硬度在靠近交界面的膜中达到最大值,最大值随着氧化时间的增加而增加。硬度曲线表现出明显的分层结构,氧化膜中的元素分别也表现出明显的分层结构;

5) MAO 处理样品的高温抗氧化性能高于基体,热氧化速度只有基体的 1/3。

参　考　文　献

[1] 李成功,傅恒志,于　翘. 航空航天材料[M]. 北京:国防工业出版社,2002:84.

[2] Diaz P, Ralph R, Edirisinghe M J. Transmission electron microscope characterization of a plasma-sprayed ZrO_2-Y_2O_3-TiO_2 thermal barrier coating[J]. Materials Characterization, 1998, 41: 55 - 67.

[3] 邵得春,李　鑫,刘克勇. 激光表面合金化提高钛合金高温抗氧化性能的研究[J]. 中国激光,1997,24(3):281 - 284.
SHAO De-chun, LI Xin, LIU Ke-yong. Improvement in resistance to high temperature oxidation of titanium alloy by laser surface alloying with Al + Nb[J]. Chinese Journal of Lasers, 1997, 24(3): 281 - 284.

[4] 唐兆麟,王福会,吴维岌. 涂层对 TiAl 金属间化合物抗循环氧化性能的影响[J]. 中国有色金属学报,1998,8(1):56 - 60.
TANG Zhao-lin, WANG Fu-hui, WU Wei-tao. Effect of coatings on cyclic oxidation resistance of TiAl intermetallics[J]. The Chinese Journal of Nonferrous Metals, 1998, 8(1): 56 - 60.

[5] 刘道新,陈　华,何家文. 等离子渗氮与喷丸强化复合改进钛合金抗微动损伤性能[J]. 材料热处理学报,2001,22(3):50 - 54.
LIU Dao-xin, CHEN Hua, HE Jia-wen. The effect of plasma nitriding and shot peening on the fretting damage resistance of Ti alloy[J]. Trans Mater Heat Treat, 2001, 22(3): 50 - 54.

[6] Kaestner P, Olfe J, Rie K T. Plasma-assisted boriding of pure titanium and TiAl6V4[J]. Surf Coat Technol, 2001, 142 (8): 248-252.

[7] Yerokhin A L, Lyubimov V V, Ashitkov R V. Phase formation in ceramic coatings during plasma electrolytic oxidation of aluminum alloys[J]. Ceramics International, 1998, 24(1): 1 - 6.

[8] Nie X, Leyland A, Song H W, et al. Thickness effects on the mechanical properties of micro-arc discharge oxide coatings on aluminum alloys[J]. Surf Coat Technol, 1999, 116: 1955 - 1060.

[9] Xue W, Deng Z, Chen R, Zhang T. Growth regularity of ceramic coatings formed by microarc oxidation on Al-Cu-Mg alloy[J]. Thin Solid Films, 2000, 372: 114 - 117.

[10] Xue W, Wang C, Chen R, et al. Structure and properties characterization of ceramic coatings produced on Ti-6Al-V alloy by microarc oxidation in aluminate solution[J]. Mater Lett, 2002, 52: 435 - 441.

[11] Verdier S, Boinet M, Maximovitch S, Dalard F. Formation, structure and composition of anodic films on AM60 magnesium alloy obtained by DC plasma anodizing[J]. Corrosion Science, 2005, 47: 1429 - 1444.

[12] 唐兆麟,王福会,吴维岌. 微弧氧化处理对 TiAl 合金抗氧化性的影响[J]. 中国有色金属学报,1999,9(Suppl.1):63 - 68.
TANG Zhao-lin, WANG Fu-hui, WU Wei-Tao. Effect of microarc oxidation treatment on oxidation resistance of TiAl alloy[J]. The Chinese Journal of Nonferrous Metals, 1999, 9(Suppl.1): 63 - 68.

[13] 薛文斌,王　超,陈如意,李永良. ZL101 铸造铝合金微弧氧化陶瓷层的组织和性能[J]. 材料热处理学报,2003,24(2):20 - 23.
XUE Wen-bin, WANG Chao, CHEN Ru-yi, LI Yong-liang. Structure and performance of Ceramic coating deposited on ZL101 casting aluminum alloy by microarc oxidation[J]. Trans Mater Heat Treat, 2003, 24(2): 20 - 23.

[14] 莫　畏,邓国珠,罗方承. 钛冶金[M]. 北京:冶金工业出版社,2002.

$CaCO_3$ by corrosion and deposition. Due to strong bonding to the matrix, the compact structure and lack of ionic selectivity permeation passage, the thickness of scale stops increasing and is kept stable since it forms at 48 hours. It is verified by electrochemical impedance spectroscopy that the corrosion scale has good coverage on the matrix and can protect it very well.

Key words: CO_2 corrosion; supercritical fluid; CO_2 corrosion-deposition scales; electrochemical impedance spectroscopy (EIS)

Effects of T6I6 temper on microstructure and mechanical properties of 2195 Al-Li alloy

YU Li-jun, ZHENG Zi-qiao, LI Shi-chen, LIU Gang, WEI Xiu-yu (School of Materials Science and Engineering, Central South University, Changsha 410083, China)

Trans Mater Heat Treat, 2006, 27(5): 79～83, figs 7, tabs 1, refs 13.

Abstract: Effects of T6I6 temper on the microstructure and mechanical properties of 2195 alloy were investigated. Results show that fracture toughness of the 2195 alloy depends on the amount, size and distribution of precipitates in this alloy with T_1 precipitate being the primary contributor. On the other hand, at the same level of strength, T6I6 temper results in considerably higher ductility and fracture toughness than those in 2195 alloy treated by T6 temper. TEM analysis reveals that the T6I6 treatment can greatly suppress the precipitation of T_1 phase at subgrain boundaries and promote the precipitation of large amount of fine T_1 and θ' phase in grains.

Key words: 2195 alloy; T6I6 temper; ductility; fracture toughness

Effect of ingots pre-treatment on microstructure and mechanical properties of extruded AZ91D tube

YU Bao-yi, BAO Chun-ling, SONG Hong-wu, LIU Zheng, YU Hai-peng (School of Materials Science and Engineering, Shenyang University of Technology, Shenyang 110023, China)

Trans Mater Heat Treat, 2006, 27(5): 84～86, figs 3, tabs 3, refs 7.

Abstract: The effect of ingots pre-treatment on microstructure and mechanical properties of extruded AZ91D magnesium alloy tube was studied. The results show that finer and equiaxed grains of the ingot are obtained and some cast defects in ingot are eliminated after pre-extrusion, which enhanced the yield strength by 15.72% and elongation by 170% for the extruded tube, respectively. After solution and aging treatment, β-$Mg_{17}Al_{12}$ well-distributed precipitates from α-Mg solid solution and the grain size becomes a little coarser in the ingot, which causes the decrease of tensile strength of extruded tube by 14MPa. In the extruded tube, whose ingot was pre-extrusion + solution aging + solution treated, the grains are greatly refined and the second phase achieved an even and disperse distribution in the matrix because of twice solution, which has greater solution strengthening effect than first solution and tensile strength enhanced by 7.5%. Meantime, combination of twice solution and pre-extrusion on the ingot remarkably increases the elongation of extruded tube by 345% as well.

Key words: magnesium alloy; extruded tube; ingots pre-treatment; microstructure and mechanical properties

Microstructure and wear resistance of laser clad NiTi/Ni_3Ti intermetallic composite coating

LI Ang, WANG Hua-ming (Laboratory of Laser Materials Processing and Manufacturing, School of Materials Science and Engineering, Beihang University, Beijing 100083, China)

Trans Mater Heat Treat, 2006, 27(5): 87～90, figs 6, tabs 0, refs 9.

Abstract: Wear-resistant NiTi/Ni_3Ti intermetallic composite coating was fabricated on substrate of a titanium alloy BT20 by laser cladding. Microstructure of the NiTi/Ni_3Ti intermetallic composite coating was characterized and the room-temperature dry sliding wear-resistance was evaluated coupling with hardened bearing steel GCr15. The coating has a homogeneous microstructure and is metallurgically bonded to the titanium alloy substrate. Wear-resistance of the composite coating is superior to BT20 titanium alloy under dry sliding wear test conditions. The excellent wear resistance of the laser clad NiTi/Ni_3Ti intermetallic composite coating is attributed to the combination of high strength and toughness of intermetallics of NiTi and Ni_3Ti.

Key words: laser cladding; intermetallics composite coating; microstructure; wear

Effects of electrolyte parameters on black ceramic coatings prepared by micro-arc oxidation of aluminum alloy

LIANG Ge, ZHAO Ren-bing, JIANG Bai-ling (School of Material Science and Engineering, Xi'an University of Technology, Xi'an 710048, China)

Trans Mater Heat Treat, 2006, 27(5): 91～94, figs 3, tabs 2, refs 9.

Abstract: The black ceramics coating was obtained through micro-arc oxidation on 6061 aluminum alloys in the phosphate solution containing NH_4VO_3. The influences of NH_4VO_3 concentration, and solution temperature on wear resistance, surface roughness, adhesion, blackness and thickness of the ceramic coatings were studied. The results indicate that with increasing of NH_4VO_3 content, the coating become blacker, the adhesion of the coatings reduce. The roughness of the coatings first reduces, and then increases, the wear resistance and coating thickness first increas and then reduce. Increasing solution temperature, the roughness and blackness of the coatings reduces, the adhesion of the coatings increases, and the coating thickness first increases and then reduces. When the NH_4VO_3 concentration is 5-8g/l and the solution temperature is 40℃, the coating displays excellent properties.

Key words: black ceramic coating; micro-arc oxidation; blackness

Characteristics of coatings fabricated by microarc oxidation on TiAl intermetallic compound

LI Xi-jin[1], CHENG Guo-an[1], XUE Wen-bin[1], ZHENG Rui-ting[1], WU Xiao-ling[1], CHENG Yun-jun[2] (1. Department of Materials Science and Engineering, Beijing Normal University; Key Laboratory of Beam Technology and Material Modification of Ministry of Education, Beijing 100875, China; 2. Research Center of Ti-Al Intermetallic Compound, High Temperature Material Research

Division , General Iron and Steel Research Institute , Beijing 100081 , China)

Trans Mater Heat Treat , 2006 ,27(5) :95～99 ,figs 7 ,tabs 0 ,refs 14.

Abstract: Ceramic coatings on TiAl intermetallic compound were fabricated by AC microarc oxidation. The variation of current density and coating thickness with time was discussed in detail. The morphology, microstructure and microhardness of the coatings were analyzed. The coating consists of three layers and good adhesion between the coating and substrate is observed. XRD analysis indicates that the different layers in the coating mainly consists of Rutile-TiO_2 and Al_2TiO_5. The microhardness of the coating increases with increasing the MAO treating time , and its maximum value in the coating locates at about 10μm from the interface. After isothermal oxidation at 1100 ℃ for 100h , the formation of Al_2O_3 revealed by XRD enhances the oxidation resistance of TiAl. It is shown that the oxidation resistance of the microarc oxidized sample is about three times higher than that of the substrate.

Key words: microarc oxidation; TiAl; microhardness; isothermal oxidation

Influence of bias voltage on morphology, phase and wear performance of magnetron sputtered CrTiAlN coatings

BAI Li-jing[1,2] , ZHANG Gui-jun[2] , JIANG Bai-ling[2] (1. School of Material Science and Engineering , Xi'an Jiaotong University , Xi'an 710049 , China ; 2. School of Material Science and Engineering , Xi'an University of Technology , Xi'an 710048 ,China)

Trans Mater Heat Treat , 2006 ,27(5) :100～103 ,figs 6 ,tabs 0 ,refs 9.

Abstract: The effect of bias voltage on morphology , phase components and wear performance of CrTiAlN coating , which was deposited by closed field unbalanced magnetron sputtered ion plating technique , was studied. The results show that the morphology and phases of the coating as well as the tribological parameters such as fiction coefficient , hardness , adhesion and wear rates of the coating are varied with bias voltage. The minimum wear rate of the coating prapared in bias voltage of - 75V is obtained. And the conclusion can be obtained that the key factor which the influences the wear performance of the coating is not its morphology but the phase components when the bias voltages are in the range of - 65V to - 85V.

Key words: bias voltage; CrTiAliN coating; morphology; phase; tribological performance

Study on process of multi-element permeation on cast steel surface

ZHOU Hai , CHEN Fei , YAO Bin , LÜ Jun-xia , GONG Wei , HU Peng-jie (Department of Mechanical Engineering , Beijing Institute of Petro-Chemical Technology , Beijing 102617 , China)

Trans Mater Heat Treat , 2006 ,27(5) :104～107 ,figs 6 ,tabs 2 ,refs 9.

Abstract: Multi-element permeation on cast steel ZG15 at lower temperature was carried out. The microstructure and hardness of alloying layer were investigated by SEM and HMV-1T micro hardometer. The influence of permeating temperature and time on thickness and micro-hardness of alloying layer was discussed. The results show that the permeated alloying layer formed on the cast steel surface consists of carbide , nitride. The hardness of the alloying layer is between 300-700HV , which depends on the process parameters. Temperature and holding time are main factors affecting the microstructure and hardness of the alloying layer.

Key words: cast steel; multi-element thermochemical treatment; micro-hardness

Enhancing corrosion resistance of AISI 316L steel surface alloyed with Ti by high current pulsed electron beam

ZHANG Ke-min[1] , ZOU Jian-xin[1,2] , YANG Da-zhi[1] (1. State Key Laboratory of Materials Modification by Ion , Laser and Electron Beams , Department of Materials Engineering , Dalian University of Technology , Dalian 116024 , China ; 2. Laboratoire d'Etude des Textures et Applications aux Materiaux (LETAM , UMR-CNRS 7078) , Universite de Metz , Ile du Saulcy , 57012 Metz , France)

Trans Mater Heat Treat , 2006 ,27(5) :108～113 ,figs 6 ,tabs 1 ,refs 24.

Abstract: The rapid surface alloying of AISI 316L stainless steel by high current pulsed electron beam (HCPEB) was investigated. A fine Ti powder layer was pre-coated on the substrate and then post-treated with HCPEB. Due to the rapid surface heating , melting , mixing and enhanced diffusion effects , part of the Ti coating was dissolved into the substrate , forming a Ti-rich layer on the top surface. Since the addition of Ti favors the formation of α phase , the alloyed layer contains a mixture of α and γ phases. Potentiodynamic tests in the simulated body fluid show that the corrosion resistance of AISI 316L stainless steel can be effectively improved after HCPEB surface alloying with Ti.

Key words: high current pulsed electron beam (HCPEB) ; surface alloying ; corrosion resistance ; stainless steel

Oxidation behavior of Ni-ZrO_2 nano-composite electroforming deposits at high temperature

ZHANG Wen-feng[1,2] , ZHU Di[1] (1. College of Mechanical and Electrical Engineering , Nanjing University of Aeronautics and Astronautics , Nanjing 210016 , China ; 2. Department of Mechanical and Electrical Engineering , Suzhou Vocational College , Suzhou 215011 , China)

Trans Mater Heat Treat , 2006 ,27(5) :114～117 ,figs 5 ,tabs 1 ,refs 11.

Abstract: The oxidation kinetics of Ni electroforming deposits and Ni-ZrO_2 composite electroforming deposits were evaluated by batch cyclic oxidation. SEM was used for the examination of surface and cross-section morphology of Ni electroforming deposits and Ni-ZrO_2 composite-electroforming deposits , and the component distribute in cross-section of composite electroforming deposits were analyzed. The results indicate that composite electroforming deposits exhibit an excellent oxidation resistance at high temperature. The oxidation film of composite electroforming deposits has a smooth surface and compact microstructure. Due to thinner oxidation film and lower internal stress ,